Gamma irradiation impact on the morphology and thermal blooming of soda-lime glass

Cite as: AIP Conference Proceedings **2290**, 050038 (2020); https://doi.org/10.1063/5.0031473
Published Online: 04 December 2020

Abdulameer Imran, Sattar Jabbar Bader, Abdalrahman Al-Salihi, and Hussain A. Badran

Gamma Irradiation Impact on the Morphology and Thermal Blooming of Soda-Lime Glass

Abdulameer Imran[1], Sattar Jabbar Bader[1,a)], Abdalrahman Al-Salihi[2] ,Hussain A. Badran[1,b)]

[1]*Physics Department, Education College for Pure Sciences, Basrah University, Basrah, Iraq*
[2]*Department of Basic Sciences, College of Dentistry, University of Basrah, Basrah, Iraq*

[a)] Corresponding author: sattarald@gmi.com
[b)]badran_hussein@yahoo.com

Abstract. Soda–lime glass was examined as a dosimeter for substantial gamma (γ) radiation doses by estimating the changes affected as a result in the range of 320–800 nm in optical absorbance at room temperature. Observation concluded that absorbance expanded with the expanding gamma doses absorbed. Dynamics of morphology and the optical aspect of irradiation glasses were examined by utilizing absorption spectra and relaxation spectroscopy. UV–Vis spectroscopy was used to record optical absorption spectra. According to the spectra of optical absorption, optical band gap, the cutoff wavelength, refractive record, and Urbach energy were resolved and identified with the auxiliary variations in the glass frameworks by various gamma dosages. In the blooming exploratory setup, a 532 nm CW laser was utilized as an excitation source. The experimental results showed that the thermal diffusivity value of Soda–lime glass increases when the gamma (γ) radiation doses increased.

Keywords: Gamma-ray, dose-response, dose rate, Urbach energy, Thermal lens,

INTRODUCTION

Soda–lime glass is widely recognized as the utmost business-tier glass. It is similarly modest and recyclable. A regular piece of soda–lime glass is 70-75 wt% SiO_2, 12-16 wt% of Na_2O, and 10-15 wt% CaO. A little level of different reagents can be included for application prerequisites and explicit properties. The important expansion in such a type of glass, besides silica (SiO_2), is sodium oxide (soda (Na_2O)). Because of their generally basic arrangement and simple accessibility and preparing, vitreous material is regularly utilized as a model to consider the material science of shapeless solids. Photonics materials of high third nonlinear optical characteristics have given vital data in applications of the optical data storge, taking all things together such as optical exchanging gadget in the optical media transmission scope [1]. Host glasses, like soda-lime glass, contain novel properties, for example, low phonon energy, highly refractive record, and extensive third-order nonlinear powerlessness that along with the nearness of other adjusted lattices were built up to upgrade the conductivity of electricity, the relaxation quality, and visual characteristics of the glass frameworks [1–3]. Optical glasses with extensive nonresounding nonlinear refractive (n_2) lists pose high potential for materials for all-optical exchanging gadgets and could be utilized to upgrade the execution of mode-lock strong state laser [4]. Enhancing the physical and visual properties of soda–lime doped inorganic glasses got much enthusiasm owing to their potential applications in optical gadgets and laser innovation [5].

The point of this examination is to explore the utilization of the soda–lime glass for γ beam dosimetry through the impacts of induced harm on the light assimilation of the glass. The examples were portrayed through TEM, morphological, surface profile, thermal blossoming, and UV–Vis spectrophotometer exploratory estimations.

The 8th International Conference on Applied Science and Technology (ICAST 2020)
AIP Conf. Proc. 2290, 050038-1–050038-9; https://doi.org/10.1063/5.0031473
Published by AIP Publishing. 978-0-7354-4020-3/$30.00

RESULTS AND DISCUSSION

Optical behaviors

Test samples were cut from glass slides of 300 μm thicknesses, the samples with 1x2cm^2 regions were lighted at various gamma beam doses. Before utilizing, the samples were cleaned with Aston solvent and the drying process was expedited with delicate tissues. The beam of gamma light was casted by utilizing a ^{137}Cs source with an introductory rate of 0.56 Gy/min. A spectrophotometer mark (CE-7200) was used to record the optical absorption spectra, provided from CECIL England. Presentation of strong materials to ionizing radiation, (gamma radiation, x-beam, alpha and beta particles, etc.) induces alterations in the miniaturized scale auxiliary characteristics, thusly influencing electrical, optical, and other physical elements of the strong materials [6,7]. The wavelength reliance 320–800 nm of the optical absorbance spectra of glass at various gamma doses is shown in figure 1. The optical assimilation spectra of the examined glass tests were recorded at room temperature. Figure 1 shows that edge of absorption is not pointed, affirming the polished period of the presented samples. The absorption frame stretches out to the unmistakable district, showing extremely solid absorption in the ultraviolet area. A somewhat move to the longest wavelength was seen alongside an increment of gamma dose. It is clear from figure 1 that the estimation of absorbance increment with the radiation dose up to 51 kGy; obviously, the optical absorption phantom circulation is almost touching to the radiation impact.

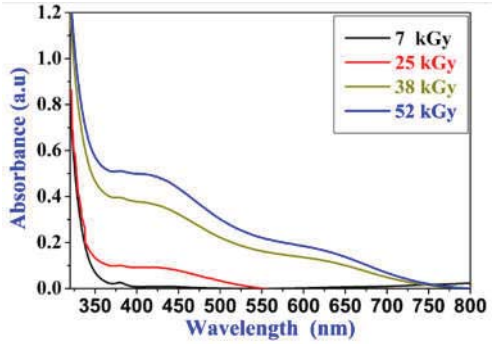

Figure 1. UV-VIS Spectrum of Soda–lime glass.

It is certain that ionizing radiation causes auxiliary imperfections (called shading focus) prompting their thickness to change on the presentation to gamma beams [8,9]. The dose reaction of the optical absorbance was contemplated over the dose scope 0-52 kGy of gamma radiation ^{137}CS.

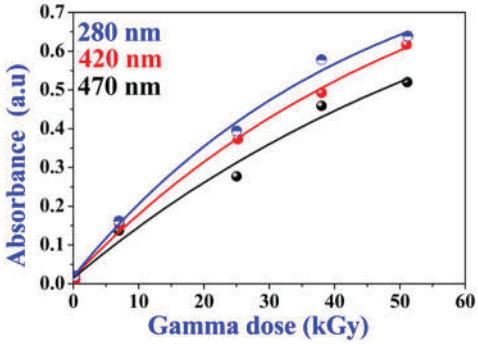

Figure 2. Variation of Absorbance with Gamma Dose.

From figure 2 it is evident that the absorbance increments straightly at 280,420, and 480 nm with ingested the dose of gamma rays up to 51 kGy after that. The change is nonlinear for sample immersion impacts at higher dosage which decreases affectability, consequently limiting samples' utility to the previously mentioned range. The base noticeable dose was observed to be 0.2 kGy. The surface morphology was analyzed by a nuclear power microscopy (AFM-Digital Instruments NanoScope). The optical absorbance and transmittance estimation increase with normal roughness. There are essential applications for roughness parameters in nonlinear and direct optics, for example,

straight electro-optical impact and optical channels and stockpiling gadgets. The morphology of the Soda–lime glass is portrayed by the picture handling. It is utilized to mimic an optical strategy to gauge the roughness of the surface, as shown in figures 3 and 4: Two typical morphological highlights are perceived promptly by visual examination of figure4. The first is that the granular highlights of different scales existing in the film and are conveyed equally in certain extents. Also, the granular highlights have various sporadic shapes, sizes, and detachments. No conspicuous accumulation was seen in the sample.

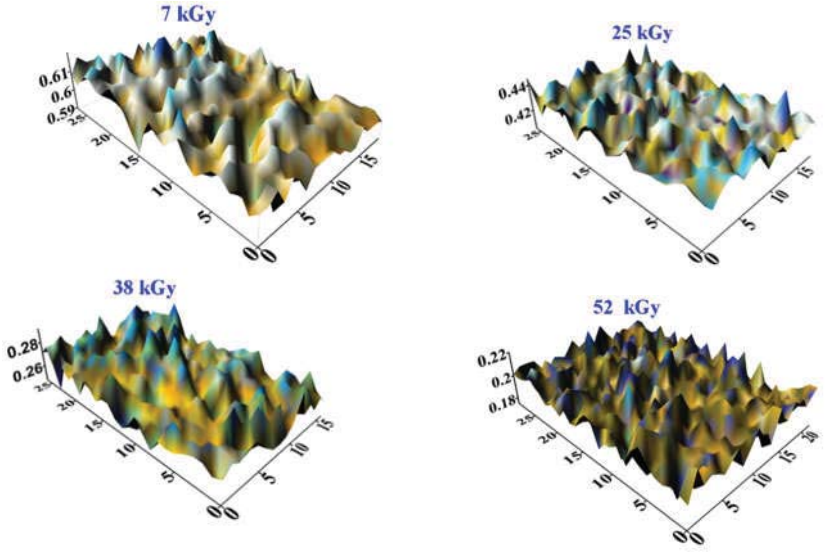

Figure 3. 3D Micrographs of the soda–lime glass with various gamma doses.

The optical band gap was acquired from the absorption spectrum data which in turn was derived from ultraviolet-visible analysis using the Davis and Mott expression for the absorption coefficient $\alpha(\nu)$ as follows [10,11]:

$$\alpha(\nu) = B\frac{(h\nu - E_g)^n}{h\nu} \quad (1)$$

Where E_g is the indirect optical band gap and n is a number, with n = 2 for allowed indirect transitions and B is a constant. $\alpha(\nu)$'s value is the absorption coefficient obtained using the following equation [12]:

$$\alpha(\nu) = 2.303\frac{A}{t} \quad (2)$$

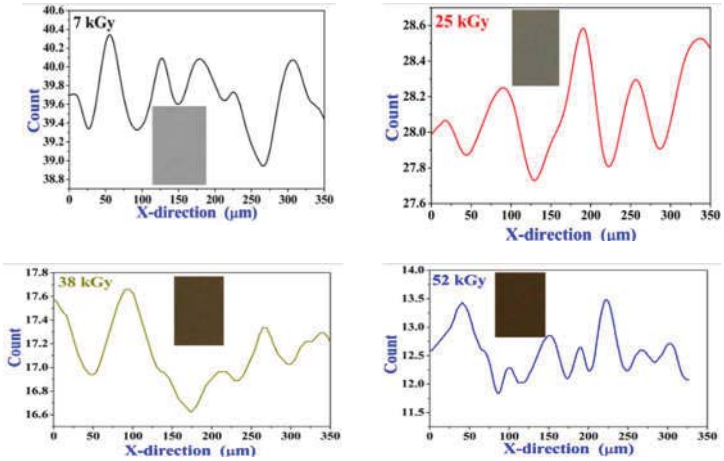

Figure 4. X-Direction Surface Profile. *Insent* One-Dimensional Optical Microscopic Image Surface.

where t is the value for the thickness of the sample and A represents the corresponding optical absorbance. Between $(\alpha h\nu)^{1/2}$ and $h\nu$, Tauc's plots were drawn. The E_g has been calculated using the plot$(\alpha h\nu)^{1/2}$ versus the visible light photon energy,$h\nu$, from the linear extrapolation to zero ordinate the calculated values of optical band gap [13,14]. The obtained data are presented in table 1. The degree of disorder in the materials was studied via Urbarch energy, represented byE_u.Materials of a higher value of $E_u$tend to convert the weak bonds into defects. As a result to possible fluctuations in the disordered material, the band tail alongside the valence and conduction bands are developed, extending into the energy gap and usually exhibiting an exponential behavior. The band tails are distinguished by a band tailing parameter and Urbach energy, E_u, given by [15]

$$\alpha(\omega) = B\, exp(\hbar\omega/E_u) \tag{3}$$

where$B$ is a constant andE_u is the band tailing parameter. Urbach energy (E_u) is deduced from the reciprocal of the graph slope of the logarithm of absorption coefficient (lnα) in contrasting comparison to the photon energy $h\nu$ [16,17]. The calculated values of Urbach energy and band gap were illustrated in figure 5. The values of$E_u$are within the range of 0.16-0.75 eV. Such a relatively small range of E_u is a result of indirect transition of phonon-assisted energy. It is given that the elevation of extinction levels at the level of absorption is heavily affected by the random internal electric field owing to absence of long-range order and present flaws in the network of the glass [17]. It was concluded that the optical band gap energy diminishes with the surge of gamma doses, contrary to Urbach energy which correlates positively to gamma doses increase. Refractive index matching the optical band gap of the examined glass samples was determined via [18],

$$\frac{n^2-1}{n^2+1} = 1 - \sqrt{E_g/20}. \tag{4}$$

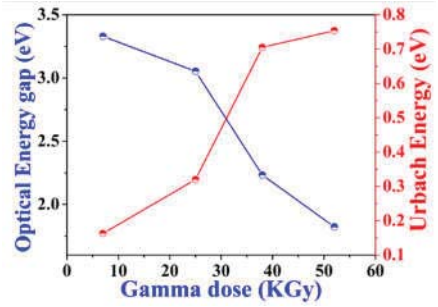

Figure 5. Urbach Energy and Optical Band Gap via Gamma Doses

The small increment of the values of the refractive index, evident in table 1, is affected by the increasing gamma doses. The small observable variation of the refractive index denotes no substantial variations in the basic commercial network of the glass with the increase in gamma dose.

Transmission Coefficient

We can obtain the transmission coefficient (T) via [19],

$$T = \frac{2n}{n^2+1} \tag{5}$$

Figure 6 plotting the correlation between reflection loss and the transmission coefficient exhibits a partially proportionally inverse correlation between both quantities [20].

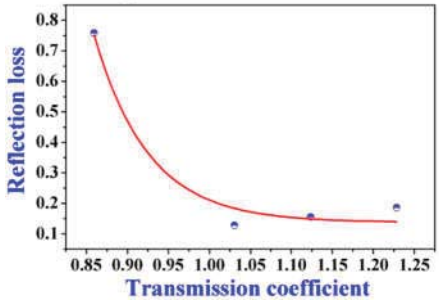

Figure 6. Reflection loss via Transmission Coefficient

Optical Susceptibility

The expanse of polarization density P effects nonlinear optical phenomena through the power series of electric field E as evident in the following expression [21]:

$$p = p^{(1)} + p^{(2)} + p^{(3)} + \ldots\ldots\ldots\ldots\ldots \quad (6)$$

$$\text{or} p = \chi^{(1)}E + \chi^{(2)}E + \chi^{(3)}E + \ldots\ldots\ldots\ldots\ldots \quad (7)$$

Where $\chi^{(1)}$ represents linear optical susceptibility and $\chi^{(2)}$ and $\chi^{(3)}$ represent the nonlinear optical susceptibility of both second and third orders. In this association, nonlinear optical glasses have pulled in substantial consideration on accounting for their significance for the advancement of optical information preparing innovations [22]. Therefore, glasses of higher optical nonlinearity must be prepared or planned according to connection of miscellaneous electronic characteristics with the optical nonlinearity that is justifiably impactive and open. As the optical nonlinearity is brought about by electronic polarization of the glass upon introduction to exceptional light pillars, polarizability is a standout amongst the utmost essential inherent aspects that administer the nonlinearity reaction of glass. The third-order nonlinear susceptibility χ^3 of soda–lime glass was estimated by generalized Miller's rule [23]:

$$\chi^{(3)} = \left[\chi^{(1)}\right]^4 .10^{-10}, esu \quad (8)$$

Where $\chi^{(1)}$ is the linear electric (dielectric susceptibility) measuring the material's capacity for transience or complete polarization, calculated by [24]:

$$\chi^{(1)} = \frac{\varepsilon - 1}{4\pi} \quad (9)$$

where ε is the dielectric constant. The acquired information is exhibited in table 1, section 5. Soda-lime glasses show high estimations of the third-order nonlinear optical vulnerability in the 0.27-32.43x10^{-13}esu territory, which is around multiple times bigger than that of unadulterated silica-glass (2.8x10^{-14}esu). This implies soda-lime glasses are likely great resources for nonlinear optical applications. As of late, point-by-point examination was conducted on the connection between electronic oxide particle polarizability and third nonlinear optical defenselessness of various glasses [21]. It was surmised that third nonlinear optical vulnerability of the glasses increments with expanding irradiation dose, electronic oxide particle polarizability that is optical basicity. This is related to the high refractive index. In this association, we have plotted the information of the $\chi^{(3)}$ as an element of refractive record number of soda-lime glasses in figure 7. It is seen that it increments with the expanding of the refractive record and gamma radiation.

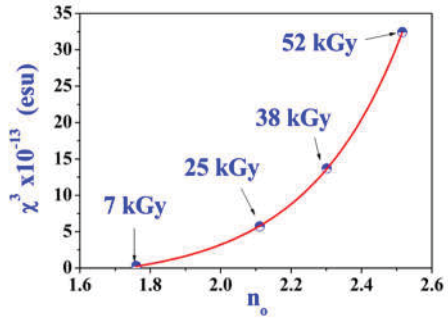

Figure 7. $\chi^{(3)}$ as a Function of the $n_{\circ}$

Table 1. Linear and Nonlinear Optical Properties of Soda–Lime with Various Gamma Doses

Dose (kGy)	$n_{\circ}$	$\chi^{(1)}$	ε	T	ε_{opt}	$\chi^{(3)} \times 10^{-13}$ esu	E_g (eV)
7	1.76	0.167	3.09	0.859	2.097	0.77	3.3
25	2.11	0.275	4.45	1.030	3.456	5.73	3.054
38	2.30	0.342	5.29	1.123	4.295	13.68	2.233
52	2.51	0.424	6.33	1.228	5.330	32.43	1.823

THERMAL BLOOMING

The trial thermal blooming setup was set up as indicated by Ref.[25].The soda–lime glass with 52 kGy gamma radiation was set up as the reference nonlinear material in the analysis. The mechanical assembly comprises a solitary transistor–transistor logic (TTL) tweaked laser light emission diode laser 11mW yield, shaft span 1.5 mm at, 532 nm wavelength, a positive glass lens of +50 mm central length, two power meters to quantify input and transmitted yield beam controls through the cell, a recurrence generator show (EM1634), and an oscilloscope display (lodestar - MOS-620CH). The laser's yield is adjusted at 20 Hz for the thermal blooming estimation.

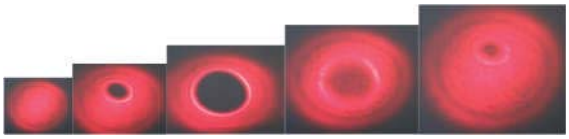

Figure 8. Blooming shapes for Soda–Lime Glass with 52 kGy Gamma Radiation

An essential trial method for a thermal blossoming estimation is to utilize a laser light emission centered-recurrence utilizing a long central-length lens and after that allowed growth. The soda–lime glass is found at one Rayleigh length right after the central plane. Rayleigh length Z_R = 5.15 mm is an indication of the depth focus. It is given by 635 nm laser wavelength with 4mW, which is 32.27 μm, is the trademark prerequisite of the power dissemination in the central plane, which for a TEM_{00} Gaussian shaft is corresponding to sample [25], where r represents the outspread separation from the beam's access. Thermalth produced in assimilation area builds up the nearby temperature, along these lines altering the refractive list and actuating an optical lens, probably separating or merging according to the indication of ∂n=∂T, indicating the temperature coefficient of refractive index of the medium. Most samples' negative lens indicate an increase in heating [26]. As the territory blossoms, the photocurrent decreases as indicated by the articulation [27]:

$$\frac{I(x,t)-I(x,t=\infty)}{I(x,t=\infty)} = \frac{\left[1-\frac{\theta}{2}tan^{-1}\left[\frac{2x}{3+x^2+(9+x^2)(t_c/2t)}\right]\right]^2}{\left[1-\frac{\theta}{2}tan^{-1}\left[\frac{2x}{3+x^2}\right]\right]^2} - 1 \qquad (10)$$

Where$I(x,t)$ represents the calculated intensity at the center of the beam, $I(x,t=\infty)$illustrates the intensity at the detector after allowing enough time at the fulfillment of a steady-state temperature difference $x = z/z_R$and

$$\theta = \frac{p\alpha L_{eff}}{\lambda K}\frac{dn}{dT} \qquad (11)$$

Wherezrepresents the distance separating the sample and the waist of the beam,α is the coefficient of linear absorption, L_{eff}represents the sample's thickness impact, given by ($L_{eff} = (1-e^{-\alpha L})/\alpha$), [28]$P$represents the input power of the laser,Kdenotes the thermal conductivity (K=0.7W.K^{-1}.cm^{-1}) , and dn/dT is the thermooptic coefficient. Estimation begins with opening a screen situated at the central plane quickly. t_c indicate the time constant of the thermal lens can be expressed as [29]

$$t_c = \frac{{w_e}^2}{4D} \qquad (12)$$

The time constant can be investigation by fitting the experimental data to Eq. 10. The thermal lens creates over time of a couple of tenths of a second. During which the laser pillar might be seen as a spot on a plane found a couple of meters past the sample. The spot "sprouts" or increments in volume, which is called thermal blossoming [30,31]. A precedent is shown in figure 8. It is not really important to quantify the extent of the recognized output; a minor photodiode locator situated cautiously at the lens of the spot delivers a photocurrent relative to the intensity of the laser on the axis and hence conversely corresponding to the beam zone. The signals of Soda-lime are shown in Fig.9 for a pumping power 4 mW. The solid line correspond to the fitted data of the Equation10 to the TL experiment and the adjustable parameters are θ and t_c. The values of θ and t_c are given in Table 2. The values of D were calculated from Equations 11 and 12 with w_e=21.63 × 10^{-3} cm and shown in Table 2.

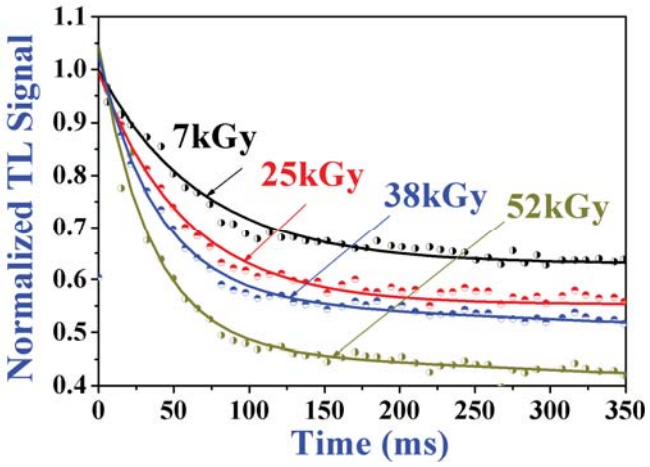

Figure 9. Experimental data and their best fit curve for Soda–lime with various gamma beams

Table 2. θ,$t_c$and Thermal Diffusivity (D) for Soda–lime with various gamma beams

Soda–lime	t_c (ms)	$\theta(rad)$	D $\times 10^{-3}$ (cm^2/sec)
7 kGy	10.2±0.02	0.25±0.003	11.46±0.02
25 kGy	9.7±0.02	0.23±0.002	12.05±0.02
38 kGy	8.3±0.01	0.31±0.001	14.09±0.01
52 kGy	7.6±0.01	0.41±0.004	15.3±0.02

CONCLUSION

Soda–lime glasses lit with various gamma beams were readied and their direct and nonlinear properties were considered. Considering optical absorbance, it is affirmed that glass is a decent material for height dosimeter applications. The rate of absorbance was within the range of 320–500 nm and was directed up to a dose of gamma radiation of 50 kGy. The diverse rate of dosage whether high are low is minimal. The direct optical properties, for example, optical band gap, diminishes from 3.33 to 1.83 eV while the refractive index increment from 1.76 to 2.516. The progressions got from E_g and the refractive record can be identified with the basic difference in the glass following irradiation with gamma beams. The third-order nonlinear optical weakness and thermal blooming got by the thermal lens method proposed that the currently considered soda–lime can be utilized for construction of all-optical exchanging gadgets. Thermal diffusivity value of Soda–lime glass increases when the gamma (γ) radiation doses increased

REFERENCES

1. C. Eevon, M.K. Halimah, A. Zakaria, C.A.C. Azurahanim, M.N. Azlan, M.F. Faznny, Results in Physics, **6** ,761–766 (**2016)**
2. Sidkey MA, El Mallawany RA, Abousehly AA, Saddeek YB. Relaxation of longitudinal ultrasonic waves in some tellurite glasses. Mater Chem Phys **2002**, 74, 222–230.
3. Abdel-Kader A, El-Mallawany R, Elkholy MM. Network structure of tellurite phosphatglasses: optical absorption and infrared spectra. J Appl Phys **1993**,73,71–74.
4. Bala R, A. Agarwal, S. Sanghi, N.Singh, Effect of Bi_2O_3 on nonlinear optical properties of ZnO. Bi_2O_3.SiO_2 glasses.Opt Mater **2013**, 36(2), 352–356.
5. K. Maheshvaran,K. Linganna,K. Marimuthu, Composition dependent structural and optical properties of Sm^{3+} doped boro-tellurite glasses J. of Luminescence **2011**,131,2746–2753
6. RL. Clough, High-energy radiation and polymers: A review of commercial processes and emerging applications, Nuclear Instruments and Methods in Physics Research Section B: Beam Interactions with Materials and Atoms, **2001**, 185, 8-33.

7. K. Arshak and O. Korosynska , Gamma radiation-induced changes in the electrical and optical properties of tellurium dioxide thin films, IEEE Sensors journal, **2003**, 3, 717-721.
8. T. M. Salman, A.Y. AL-Ahmad, H. A. Badran and C. A Emshary,Diffused transmission of laser beam and image processing tools for alpha-particle track-etch dosimetry in PM-355 SSNTDs,Phys. Scr. **2015,** 90, 085302 (8pp).
9. T.M. Salman1, R. K. Alfahed , H. A. Badran, K. I. Ajeel, M. M. Jafer and K. K. Mohammad,The evaluation and analysing the boron concentration rate in soil of north Basrah city Iraq) by (carmine method, *IOP Conf. Series:Journal of Physics: Conf. Series,* **2019**,1294**,** 022006
10. H. A. Badran, study on optical constants and refractive index dispersion of neutral red doped polymer film**,** American J. of Applied Sciences, **2012**, 9, 250-253.
11. R. K. Fakher Alfahed, K. K. Mohammad, M. S. Majeed, Hussain Ali Badran, Kamal M. Ali, Burak Yahya Kadem, IOP Conf. Series: Journal of Physics: Conf. Series **2019**, 1279, 012019
12. H.A. Badran, A. Al‐Maliki, R. K. Fakher Alfahed, B. A. Saeed, A. Y. Al‐Ahmad, F. A. Al‐Saymari, R. S. Elias, Synthesis, surface profile, nonlinear reflective index and photophysical properties of curcumin compound, J. Mater. Sci.: Mater Electron, **2018**, 29, 10890–10903.
13. H. A.Badran, K.I.Ajeel and H.G.Lazim,"Effect of nano particle sizes on the third-order optical non-linearities and nanostructure of copolymer P3HT: PCBM thin film for organic photovoltaics," Materials Research Bulletin, **2016**,76, 422- 430.
14. H. G. Lazim, K. I. Ajeel, H. A. Badran, "The photovoltaic efficiency of the fabrication of opolymer P3HT: PCBM on different thickness nano-anatase titania as solar cell, Spectrochimica Acta Part A: Molecular and Biomolecular Spectroscopy, **2015**,145,598-603
15. H.A. Badran, A.A. Al-Fregi, R.K. Fakher Alfahed, A.S. Al-Asadi, Study of thermal lens technique and third-order nonlinear susceptibility of PMMA base containing 5′, 5″-dibromo-*o* cresolsulfophthalein, J. Mater. Sci.: Mater Electron*,* **2017**,28, 17288-17296.
16. S.Insiripong, P. Chimalawong, J. Kaewkhao,P. Limsuwan, Optical and physical properties of bismuth borate glasses doped with Dy^{3+}. Am. J. Appl. Sci. **2011**, 8(6), 574-578
17. D.P. Singh, G.P. Singh, Conversion of covalent to ionic behavior of Fe_2O_3-CeO_2-PbO-B_2O_3 glasses for ionic and photonic application. J. Alloy. Compd. **2013**,546, 224–228
18. G. Keerti Marita, S. Cole, Characterization of Mn^{+2} ion doped KCdBSi (K_2OCdO-B_2O_3. SiO_2) glasses on the basis of optical and physical properties. Int. J. Sci. Res. **2013**,2(8), 77–80
19. D. Linda, J.-R. Duclère, T. Hayakawa, M. Dutreilh-Colas, T. Cardinal, A. Mirgorodsky, A.Kabadou, P. Thomas, Optical properties of tellurite glasses elaborated within the TeO_2–Tl_2O–Ag_2O and TeO_2–ZnO–Ag_2O ternary systems, J. Alloys Compd. **2013**,561, 151–160.
20. Schott Glas, Optical Glass: Description of Properties, **2000**, 55.
21. V. Dimitrov, T. Komatsu, Electronic Polarizability, Optical Basicity and Single Bond Strength of Oxide Glasses, Journal of Chemical Technology and Metallurgy, **2013**,48(6), 549-554
22. M. Yamane, Y. Asahara, Glasses for Photonics, Cambridge University Press, **2000**.
23. H. A. Badran, H. F. Hussain and K. I. Ajeel, "Nonlinear characterization of conducting polymer and electrical study for application as solar cells and its antibacterial activity, Optik, **2016**, 127, 5301-5309.
24. H. A. Badran, A.Y.Taha, A.F.Abdulkader and C.A.Emshary,"Preparation and Study of the Electrical and Optical Properties of a New Azo Dye(4-Acetaminophenol–[2-(4-Azo)]-4-AminoDipheyl Sulfone)"J.of Ovonic Research, **2012**, 8(6),161-170.
25. H.A. Al‐Hazam, R. K. Fakher Alfahed, A. Imran, H. A. Badran, H. S. Shaker, Abd- Alrahman Alsalihi, K. I. Ajeel, Preparation and optoelectronic studies of the organic compound [2‐(2,3‐dimethyl phenylamino) ‐*N*‐Phenyl benzamide doped (PMMA)], J Mater Sci: Mater Electron,**2019**, 30, 10284–10292
26. F. A. Al-Saymari, H. A. Badran, A. Y. Al-Ahmad and C. A. Emshary, Time dependent diffraction ring patterns in bromothymol blue dye doped PMMA film under irradiation with continuous wave green laser light, Indian J Phys., **2013**, 87(11), 1153–1156
27. H. Ali Badran Thermal lens and all optical switching of new organometallic compound doped polyacrylamide gel, Results in Physics, **2014,** 4, 69–72
28. R. K. Fakher Alfahed, A. S. Al‐Asadi, H. A. Badran, K. I. Ajeel, Structural, morphological, and Z-scan technique for a temperature-controllable chemical reaction synthesis of zinc sulfide nanoparticles, Applied Physics B, **2019**, 125,48

29. H. A. Badran, K. Abd. Al-adil, H. G. Lazim and A. Y. Al-Ahmad, “Thermal blooming and photoluminescence characterizations of sol–gel CdO–SiO_2 with different nanocomposite,J Mater Sci: Mater Electron, **2016**, 27, 2212–2220.
30. H. A. Badran, Thermal properties of a new dye compound measured by thermal lens effect and Z-scan technique, Appl. Phys. B, **2015**, 119, 319–326
31. H. A. Badran,“ Z-Scan Measurement for the thermo-optic Coefficient and transmitted beam Profile of 1.8-Dihydroxy- Naphthalin-3, 6 (Disulfonic Acid-[2-(4-azo)]-N-5- Methyl-3 -Isoxazolyl)-Benzene Sulfonamide,”Advances in Physics Theories and Applications,**2013,**26, 36-44.